Improving Face Detection Performance by Skin Detection Post-Processing

Oeslle Lucena*, Ítalo de P. Oliveira†, Luciana Veloso‡ and Eanes Pereira§
University of Campinas (UNICAMP)*, Federal University of Campina Grande (UFCG)†
Email: *oeslle@dca.fee.unicamp.br, †italooliveira@copin.ufcg.edu.br, ‡luciana.veloso@dee.ufcg.edu.br, §eanes@dsc.ufcg.edu.br

***Abstract*—Face detection is already incorporated in many biometrics and surveillance applications. Therefore, the reduction of false detections is a priority in those systems. However, face detection is still challenging. Many factors, such as pose variation and complex backgrounds, contribute to false detections. Besides, the fidelity of a true detection, measured by precision rate, is a concern in content-based information retrieval. Following those issues, combinations of methods are developed focusing on balancing the trade-off between hit-rate and miss-rate. In this paper, we present an approach that improves face detection based on a post-processing of skin features. Our method enhanced the performance of weak detectors using a straightforward and low complex skin percentage threshold constraint. Furthermore, we also present a statistical analysis comparing our approach and two face detectors, under two different conditions for skin detection training, using a robust dataset for testing. The experimental results showed a significant drop in the number of false positives, reducing in 53%, while the precision rate was elevated in almost 5% when the Viola-Jones approach was used as face detector.**

***Index Terms*—Face detection, Skin detection, Performance Improvement, Post-processing**

I. Introduction

Among many popular topics in object detection, detecting faces is one of the most studied subjects of research in computer vision. Many daily applications have face analysis as an important step, for instance: video surveillance, medical assistance, and human-computer interaction [1].

Optimal hit rates with low missing detections is a hard task in face detection [1] [2]. Image rotation, pose change, complicated backgrounds, and other factors contribute to raise the number of false positives [3]. To this end, combined approaches have been widely applied, and the incorporation of skin features in face detection have achieved optimal performance rates [4]–[6].

In general, the combination of skin features with face detection consists of two major approaches [7]: 1) pre-filtering or pre-processing and 2) post-filtering or post-processing skin analysis. In the first method, for an input image, the face detector is applied in regions which the human skin is already segmented. The second approach uses skin information to classify face candidates after they skin have been detected. In the last method, the skin detector works as a false positive corrector.

Usually, combined approaches to face detection are commonly done in many different color spaces, such as RGB, YUV, and YCbCr [8], or a combination of them [9]. Also, the use of morphological filtering is considered in many cases for noise-removal and to preserve the largest connected component which commonly represents the face candidates [10].

In this paper, we propose an improvement on face detection performance regarding the precision rate for weak face detectors by a skin detection post-processing. We considered here weak face detectors the ones that reach maximum detection rate with a high false detection rate, for example, the Viola-Jones face detector [11]. We adopted the post-processing combined approach which we threshold the ratio of skin pixels over the non-skin pixels under an experimental constraint. Furthemore, we chose to use the conventional RGB color space, and we did not use any morphological filtering, which usually have to fine-tune many parameters. Also, our approach differs from what is used in the literature that is based on the number of pixels in the ROI and a fine-tuned parameter [12].

Our main contributions in this work are: 1) an improvement of the precision rate for weak detectors using post-processing skin features analysis with a simple constraint; 2) a thorough experimental evaluation of our combination method for two different face detectors, using two different datasets.

This paper is organized as follows. In Section II, we review previous works that motivated our study. Next, we describe in details our method in Section III. Sequentially, experiments and results to validate the method are reported in Section IV. Finally, conclusions and future work are presented in Section V.

II. Related work

There is an extensive literature on face detection exploring skin features that is not covered in this section. We will mention here the relevant papers that most influenced our work [9], [10], [12]–[19] which are classified into two major groups: pre-filtering and post-filtering approaches. More details can be found in surveys such as Zafeiriou et al. [1].

A. Pre-filtering approaches

Kovac et al [13] proposed a human skin color for face detection. They used some heuristic rules for the skin classification. Subsequently, regions that are not likely to be face candidates are removed based on the geometric properties of a human face. This work was the first to explicitly define boundary rules for the skin segmentation.

Phung et al. [14] proposed a skin color-based face detection using a 3D clusters of Gaussian distributions in the YCbCr space for the skin color model. Mahalanobis distance from the clusters is used to classify a pixel as skin or non-skin. In this work, the authors were pioneer to use a non-parametric skin color distribution modelling.

Zou and Kamata [15] used the HSI, RGB, and YCbCr color spaces. They built a Gaussian Mixture Model to allow the illumination compensation. Their face detection algorithm deals with images with complex backgrounds using a parallel structure. To validate their system, the authors used the Caltech dataset [1]. However, such dataset has few images and the evaluation only consisted of the detection and false detection rate.

Gaussian Mixture Models in YCbCr color space are used in [16]. They pre-filtered the images using morphological filtering, eliminating small regions that correspond to noise in face candidates. Faces are detected by similarity using template matching. In this work, the authors used the GTAV dataset[2] which contains only 182 images.

Luh [17] adopted a hybrid skin color model RGB-CbCrCg and mathematical morphology filtering. They validated the face detector with the ECU dataset [20]. The system performance evaluation was based on the detection and false detection rates.

Muhammad and Abu-Bakar [9] combined two color spaces for skin detection: HSV and YCgCr generating the SCgCr color space. The face detection algorithm applies morphological filtering and edge detection to identify the boundaries of a face candidate. The authors used the Paratheepan and Bao datasets [21], [22], but they tested the algorithm only in 90 images. The adopted evaluation metrics were restricted to the detection and false detection rate. Besides, they had a very low detection rate.

Similarly, Wang et al. [10] used a morphological filtering approach after the skin detection, with different operations, in YCbCr color space. The algorithm applies a fine localization method that is comprised of component analysis, Local Iterated Conditional Modes (LICM) [23], and morphological filtering too. The authors used the Caltech face dataset, obtaining a high detection rate with few false detections. However, the method is iterative and time-consuming.

B. Post-filtering approaches

The algorithm proposed by Erdem et al. [12] differs from those previously mentioned in this paper. A skin post-filtering method is done to reduce the number of false positives and to improve the face detector precision. The authors used Bao dataset for face detection, Bayesian detector [24], and Explicitly Defined Skin Color as skin detectors. The experiments were conducted with and without illumination compensation. The images used in the paper were in RGB color space. Although they achieve high precision with low sensibility in detection rate, they used Bao dataset, which has few images and no official ground truth.

Mostafa et al. [18] also proposed a skin post-filtering method. The authors combined facial features with a skin model to reduce the false positives of the face detector. They evaluated the algorithm using exclusively the Viola-Jones [11] approach as face detector under the Face Detection Data Set and Benchmark (FDDB) [25] and LFPW databases [26].

Ban et al. [19] investigated a new method for face detection based on skin color likelihood via a boosting algorithm. They measured and compared the detection rate and false detection rate for different datasets, such as the FDDB and Bao datasets. Ban et al. [19] performed a skin post-filtering approach. Their implementation was concentrated at the Viola-Jones face detector, either using Haar-like features or LBP features.

Likewise the previously approaches, our method is based on a skin post-filtering. We implemented an algorithm using two different face detectors, which were Viola-Jones approach and Pixel Intensity Comparisons Organized in Decision Trees (PICO) [27]. Also, we exploited the FDDB dataset, which has a large set of images with different illumination and in-plane rotated faces. Besides that, we evaluated two different datasets for skin detection, which were Jones & Rehg dataset [24] and ECU database [20]. Although we did not use an illumination compensation, our results also reduced the number of false positives and improved the face detector precision using a novel constraint approach. Additionally, a significant statistical analysis is performed, involving ROC curves (Receiver Operating Characteristic), Precision, True Positive Rate (TPR), False Positive (FP), the AUC (Area Under the Curve) and F1-score.

III. Proposed Approach

The proposed method is composed of the following pipeline: (a) Face Detection, (b) Skin Detection, and (c) Skin Percentage Evaluation. Although the used pipeline was already applied in literature [12], our proposal differs in two main aspects: the threshold constraint in step (c), and the fact that we did not use morphological filtering as in [28]. The algorithm methodology is presented in Figure 1. In Figure 2, we show an example of how our method is works.

A. Face Detection

The face detection module is responsible for finding the human faces in the image. In other words, given an input image, the goal is to use an algorithm to find a region of pixels that represents a human face [29]. For this step, we used two face detectors: the Viola-Jones and the PICO.

1) Viola-Jones Face Detector: The well-known Viola-Jones [11] approach is based on boosting and integral images; its implementation was incorporated to the Open Source Computer Vision (OpenCV) library [3]. Haar Features are extracted from integral images, they are rectangular, and they represent edges, lines, borders, or other primitive structures [30]. Viola-Jones face detector uses a cascade of weak detectors. Each

[1]Available at http://vision.caltech.edu/

[2]Available at https://gtav.upc.edu/en/research-areas/face-database

[3]http://docs.opencv.org

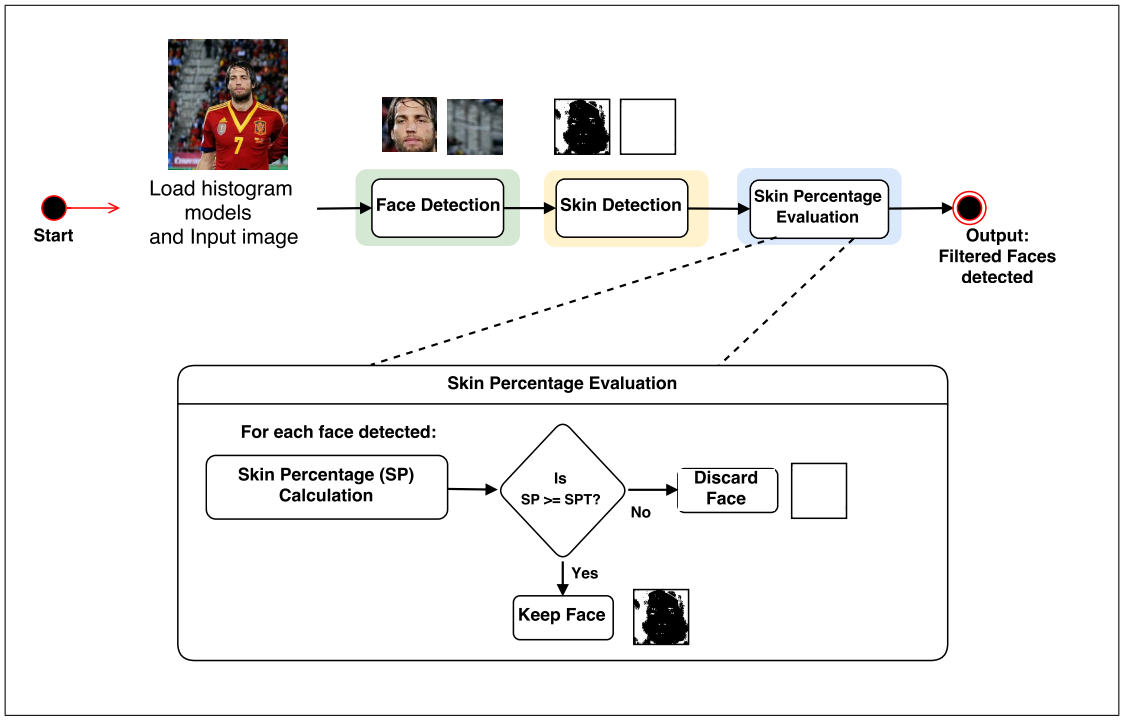

Fig. 1. Flowchart diagram of the proposed algorithm, the blank square indicates that no skin pixels were identified in the ROI.

detector is responsible for one feature, and the AdaBoost algorithm is used to combine all weak detectors into an effective detector.

2) PICO Face Detector: This face detector is a modification of Viola-Jones, being responsible for scanning an image with a cascade of binary detectors at all reasonable positions and scales [27]. Its code implementation is provided by the authors in C/C++ languages[4]. Each binary detector consists of an ensemble of decision trees with pixel intensity comparisons as binary tests in their internal nodes. The learning process consists of a greedy regression tree construction procedure and a boosting algorithm.

B. Skin Detection

For each input image, the skin detection module applies a pixel-wise classification. In this module, we built a skin detector based on statistical color models proposed by Jones et al. [24]. The algorithm performs skin classification comparing the skin and non-skin color models under a threshold Θ constraint. Basically, given a value for Θ, the skin detector checks for every pixel if the amount of skin over the amount of non-skin is greater or equal to Θ. If so, it classifies as human skin, if not it classifies as non-human skin.

Statistical color models are *RGB* histograms. The skin and non-skin color models consist in *RGB* histograms calculated from a dataset of images, which contain labeled masks for skin and non-skin pixels. Each histogram has 256 bins per channel, resulting in a 16.7 million degrees of freedom (256^3), thus, it represents a $3D$ histogram where the pixel intensity varies from black ($RGB = 0, 0, 0$) to white ($RGB = 255, 255, 255$). According to Kawulok et al. [31], the reduction of bins per channel improves the algorithm speed and promotes better histogram models. Therefore, in this work, we adopted 64 bins per channel.

As previously stated, the skin and non-skin color models are built using an image dataset. In our case, we used Jones & Rehg dataset [24] and ECU dataset [20]. Those models are computed once, and then they are used to detect skin for a new input. Afterwards, a comparison between the image and the corresponding mask is performed as follows: for each skin color that appears in the image, an increment of one is done for the correspondent bin at the skin histogram. The same process is repeated to non-skin colors in the non-skin histogram.

The skin detection problem is formalized as following: given a set of images $I = \{i_1, i_2, \ldots, i_m\}$ and a function α, such that

$$\alpha : I \rightarrow H \tag{1}$$

where $i_j = \{v_k | 0 \leq v_k \leq 255\}$, and $H = \{x | 0 \leq x \leq 1\}$. The function α computes the relative frequency distribution (RFD), $RFD = \{f_l | f_l \in H, 0 \leq l \leq 63\}$, for all pixel values, $v_k \in i_j$. Such that,

- $f_l \geq 0$
- $\sum_l f_l = 1$

In order to classify a pixel value, v_k, as being skin (or not skin), one may apply the function γ, for each $v_k \in i_j$.

[4]https://github.com/nenadmarkus/pico

Fig. 2. Example of proposed algorithm application.

$$\gamma : i_j \rightarrow Q \tag{2}$$

where $Q = \{-1, 1\}$, and 1 means is skin, -1 is not skin.

The probability of a pixel value comes from a skin (or not skin) image is given by function $\delta(v_k, Q)$, as in Equation 3.

$$\delta : (v_k, Q) \rightarrow H \tag{3}$$

where

$$\delta(v_k, 1) = \frac{(\sum_{j=0}^{m} \sum_{n=0}^{K} 1\{i_j(n) = k \wedge \gamma(v_k) = 1\})}{X} \tag{4}$$

and $1\{.\}$ is the indicator function, so that $1\{true\} = 1$ and $1\{false\} = 0$, X is the quantity of pixels in all images. In Equation 4, m is the number of images, and K is the number of pixels for each image. Similarly for not skin, the Equation 5 may be computed.

$$\delta(v_k, -1) = \frac{(\sum_{j=0}^{m} \sum_{n=0}^{K} 1\{i_j(n) = k \wedge \gamma(v_k) = -1\})}{X} \tag{5}$$

Conditional probabilities and Bayes Theorem may be applied as in Equations 6 and 7 to obtain a parametrization of the probability of occurence of a given pixel value, v_k, given the observation of it being skin, $\gamma(v_k) = 1$, or not skin, $\gamma(v_k) = -1$.

$$P(v_k|\gamma(v_k) = 1) = \frac{\delta(i_j = v_k, \gamma(v_k) = 1)}{P(\gamma(v_k) = 1)} \tag{6}$$

$$P(v_k|\gamma(v_k) = -1) = \frac{\delta(i_j = v_k, \gamma(v_k) = -1)}{P(\gamma(v_k) = -1)} \tag{7}$$

In Equations 6 and 7, $P(\gamma(v_k) = 1) > 0$ and $P(\gamma(v_k) = -1) > 0$.

Finally, the decision threshold is computed by function $\tau : (\Theta, R) \rightarrow Q$ as in Equation 8, with R being a conditional probability ratio and Θ a given threshold.

$$\tau(\Theta, R) = \begin{cases} 1 & \text{, if } R \geq \Theta, \\ 0 & \text{, if } R < \Theta. \end{cases} \tag{8}$$

In Equation 8, $R = \frac{P(v_k|\gamma(v_k)=1)}{P(v_k|\gamma(v_k)=-1)}$. If $\tau(\Theta, R) = 1$, the pixel is considered as a skin pixel, and if $\tau(\Theta, R) = 0$, the pixel is considered as a non- skin pixel.

The threshold Θ as reported by Jones and Rehg [24] is obtained by the trade-off of the correct and false detections from the ROC curve, which is a graphical plot that illustrates the performance of the detector as its threshold varies [32]. In this case, Θ is the optimal threshold value extracted from the ROC Curve.

C. Skin Percentage Evaluation

The module for skin percentage evaluation is responsible for checking whether or not a face candidate should be kept or deleted from the face candidate list based on a given skin ratio threshold (Υ). Given an image, i_j, and the previously defined functions, the decision for a given skin ratio threshold is computed by Equation 9.

$$v(i_j) = \begin{cases} 1 & \text{, if } \frac{\sum_{n=0}^{K} 1\{i_j(n)=k \wedge \tau(v_k)=1\}}{(\sum_{n=0}^{K} 1\{i_j(n)=k \wedge \tau(v_k)=0\})+\epsilon} \geq \Upsilon, \\ 0 & \text{, otherwise.} \end{cases} \tag{9}$$

where K is the quantity of image pixels, $1\{.\}$ is the indicator function, and ϵ is a small real number (e.g., 0.0000001) to guarantee that the ratio will be a real number even when there is no pixel classified as non-skin.

IV. Experiments and Results

In this section, we describe in subsection IV-A the details of how our experiments were conducted. In subsection IV-B, we detail the experimental results with a discussion of the proposed method performance, and its statistical analysis.

A. Experimental Setup

We used the FDDB dataset [25] to evaluate the performance of our method. This dataset contains 2,845 images with a total of 5,171 faces, both grayscale and color images. The ground truth is composed of manually annotated faces localized using rectangular and ellipse regions. Furthermore, since our skin detection uses RGB color space to generate the color models, we modified the FDDB dataset to fit our approach. Therefore, we semi-automatically removed all the grayscale images in the dataset and their correspondent annotated faces, resulting in 2,793 images with a total of 5,060 faces.

The experiments were conducted by fine-tuning the parameters of the modules from our algorithm. The tuned parameters were: face detector, skin train dataset and its optimal Θ, and the Υ values. For the Face Detection module, we used the two following detectors: Viola-Jones and PICO, which were described in Section III.

For the Skin Detection module, in the training phase, the experiments were carried out for two datasets, namely: Jones & Rehg dataset and ECU dataset. Jones & Rehg dataset originally contains 13,640 images with a total of 8,965 non-skin images and 4,675 skin images, and the ECU dataset contains 4,000 images. In our work, we used 6,839 images from Jones & Rehg dataset with a total of 4,511 non-skin images and 2,328 skin images and 2,000 images from the ECU dataset to generate the models. We also had to experimentally compute the optimal thresholds Θ for both datasets. The threshold is based on the trade-off of the correct and false detections from the ROC curve, which is done using different images for the training and the testing phases. In other words, to excerpt the optimal thresholds Θ it is necessary to train and test the skin detector. Later, we ended up with Θ = 0.9 using Jones & Rehg dataset and Θ = 1.3 using ECU dataset. Afterwards, the changes in this module were to select a training dataset and a threshold value for the Θ.

For the Skin Percentage module, we used the following values for Υ: 5%, 10%, 15%, 20% and 40%. Empirically, we verified that the Υ values above 40% drastically reduced the number of positive detections. That occurred because, in general, the skin pixels from the detected face occupies less than 50% in the rectangular detection from the the Viola-Jones and PICO face detectors. Thus, Υ values above 40% were not considered.

Finally, each experiment was conducted by the following procedures: 1) select a face detector, 2) select a dataset for skin detection training and a threshold value for Θ, and 3) perform the skin percentage evaluation for all Υ values. Then, we compare the results of our face detector algorithm with the original Viola-Jones and PICO face detectors. All the analysis were done using a workstation equipped with an Intel Core i7-3632QM 2.2 GHz (8 GB RAM) processor, Windows 10 Home (64 bits), and the codes were implemented in C++ language using OpenCV[5] library.

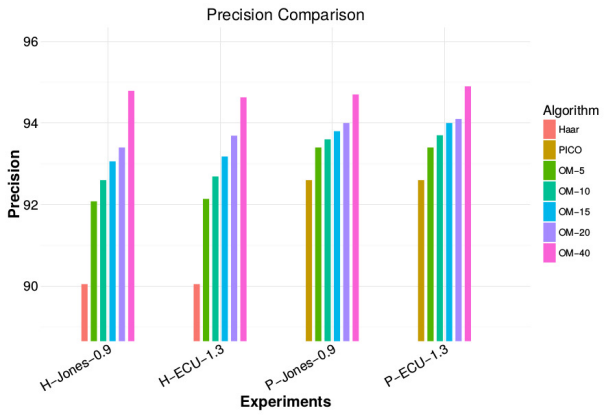

Fig. 3. Precision comparison among our method, Viola-Jones, and PICO Face detectors.

B. Results

We computed the ROC curve, TPR, FP, Precision or Positive Predictive Value (PPV), F1-score, and AUC of our experiments. Initially, we measured those rates and plot the curves for our method (OM) using the Viola-Jones, also shown as Haar or H in the Figure 3, and PICO as face detectors showed as P in Figure 3. Then, we compared the results without OM. The AUCs were measured for the best FP behaviors from OM in all cases were for Υ equals to 40%. Thus, all curves were limited to that number of FPs for this metric.

We present the statistical results of our experiments in Table I. The first row shows the reference results for the Viola-Jones and PICO face as face detectors without using OM. The other rows present the results for a specific skin dataset training and a specific Υ value. For example, ECU-OM-5 is an experiment conducted with ECU as a skin dataset training using our method with Υ equals to 5%.

The application of OM improved the PPV and reduced the number of FPs in all cases. The best values are in bold on the Table I, and the best case scenario improved the Precision rate in $\approx 5\%$ reducing in 201 the number of FPs, which represents 53% of FPs that the original detector hit. The drawback of our approach is that the improvement of the PPV reduced the TPR in the experiments. This happened because in the FDDB dataset there are very small an occluded annotated faces with only a small part of the face visible in the image [18]. Due that,

[5]http://opencv.org/

TABLE I
EXPERIMENTAL STATISTICAL RESULTS.

Face detector	Viola-Jones					PICO				
Statistics / Methods	TPR	FP	PPV	F1-Score	AUC	TPR	FP	PPV	F1-Score	AUC
Reference	67.3	376	90.1	77.0	0.53	70.1	285	92.6	**79.8**	**0.62**
ECU-OM-5	66.7	288	92.1	**77.4**	0.53	69.4	248	92.6	79.7	0.61
ECU-OM-10	66.4	265	92.7	**77.4**	0.53	69.1	235	93.4	79.6	0.61
ECU-OM-15	66.1	245	93.2	**77.4**	0.53	68.9	224	94.0	79.5	0.61
ECU-OM-20	65.8	224	93.7	77.3	0.53	68.4	219	94.1	79.2	0.60
ECU-OM-40	62.4	179	**94.6**	75.2	**0.54**	64.3	176	**94.9**	76.6	0.57
Jones & Rehg-OM-5	66.6	290	93.4	77.3	0.53	69.5	249	93.4	**79.7**	**0.62**
Jones & Rehg-OM-10	66.5	269	93.7	**77.4**	0.53	69.4	240	93.6	**79.7**	**0.62**
Jones & Rehg-OM-15	66.0	249	94.0	77.2	0.53	69.3	232	93.8	**79.7**	**0.62**
Jones & Rehg-OM-20	65.7	235	94.1	77.1	0.53	69.1	224	94.0	**79.7**	0.61
Jones & Rehg-OM-40	62.9	175	**94.9**	75.6	**0.54**	67.0	190	**94.7**	78.5	0.60

when detected, these face candidates were too small compared with the rectangular ROI drew around the face, resulting in skin percentage levels for much lower than the Υ used in this work. Therefore, they were rejected by the skin percentage evaluation.

Our method had the best AUC and F1-score along the experiments with the Viola-Jones, being very close to the original detector when the PICO was used as face detector. Thus, that confirms we had improved the performance of weak detectors.

The ROC curves are shown in Figures 4 and 5. These curves show the performance of the detectors for different face confidence thresholds and the limited curves for the AUC calculation, respectively. It is possible to see that when the number of FP increases, the performance of OM is worse than the regular face detectors. However, in the best case scenarios, when the Precision of OM is the greatest one, the behavior of the ROC curves looks like the same or have better performance than the regular face detectors.

In Figure 3 we present a bar plot comparing the Precision of the face detectors with and without OM. Each block in the graph represents the comparison of five rows for one face detector from Table I, as follows: H-Jones-0.9 indicates that was used Viola-Jones as face detector with Jones & Rehg skin dataset training, with Θ equals to 0.9. Also, each bar represents a precision value for one Υ using our algorithm.

From Figure 3 we conclude that the PPV from the experiments using OM with Viola-Jones, when compared with the reference values, were more effective than the experiments using OM with PICO. That happened because the Viola-Jones algorithm is less robust than the PICO, and therefore it is more sensitive to adjustments. Hence, the weak detectors had better performance using OM again.

Another point to consider from the bar plot graph in Figure 3 is the PPV value using Viola-Jones and Υ equals to 40% is greater than the reference PICO Precision. Thereby, using the PPV perspective, our method allows using a weak face detector with the same hit fidelity to a more robust face detector as the PICO.

V. CONCLUSION

In this paper, we introduced an improvement for face detection exploring skin features post-processing. We remark that a simple constraint was used to analyze the influence of a threshold obtained by the ratio among quantities of skin and non-skin pixels. Our experimental results showed a large drop in the number of false positives, reducing in 53%, while the precision rate was elevated in almost 5% when the Viola-Jones was used as face detector. Furthermore, we noted that weak face detector algorithms, i.e. Viola-Jones, when submitted to our method, had their precision rate greater than more robust algorithms.

Additionally, we brought a significant statistical analysis under different conditions for face detector and skin detectors, using complex datasets, such as the FDDB. For future works, we suggest employing an illumination correction algorithm and the investigation of skin detection approach based on robust features, such as Local Binary Patterns (LBP) [33].

ACKNOWLEDGMENT

The authors would like to thanks the Laboratory of Computer Perception (LPC) for supporting the implementation of this work in their facilities. Also, we thank the Federal University of Campina Grande (UFCG).

REFERENCES

[1] S. Zafeiriou, C. Zhang, and Z. Zhang, "A survey on face detection in the wild: Past, present and future," *Computer Vision and Image Understanding*, vol. 138, pp. 1 – 24, 2015.

[2] J. Galbally, S. Marcel, and J. Fierrez, "Biometric antispoofing methods: A survey in face recognition," *IEEE Access*, vol. 2, pp. 1530–1552, 2014.

[3] Q. Zhang, L. F. Zhou, W. S. Li, K. Ricanek, and X. Y. Li, "Face detection method based on histogram of sparse code in tree deformable model," in *2016 International Conference on Machine Learning and Cybernetics (ICMLC)*, vol. 2, July 2016, pp. 996–1002.

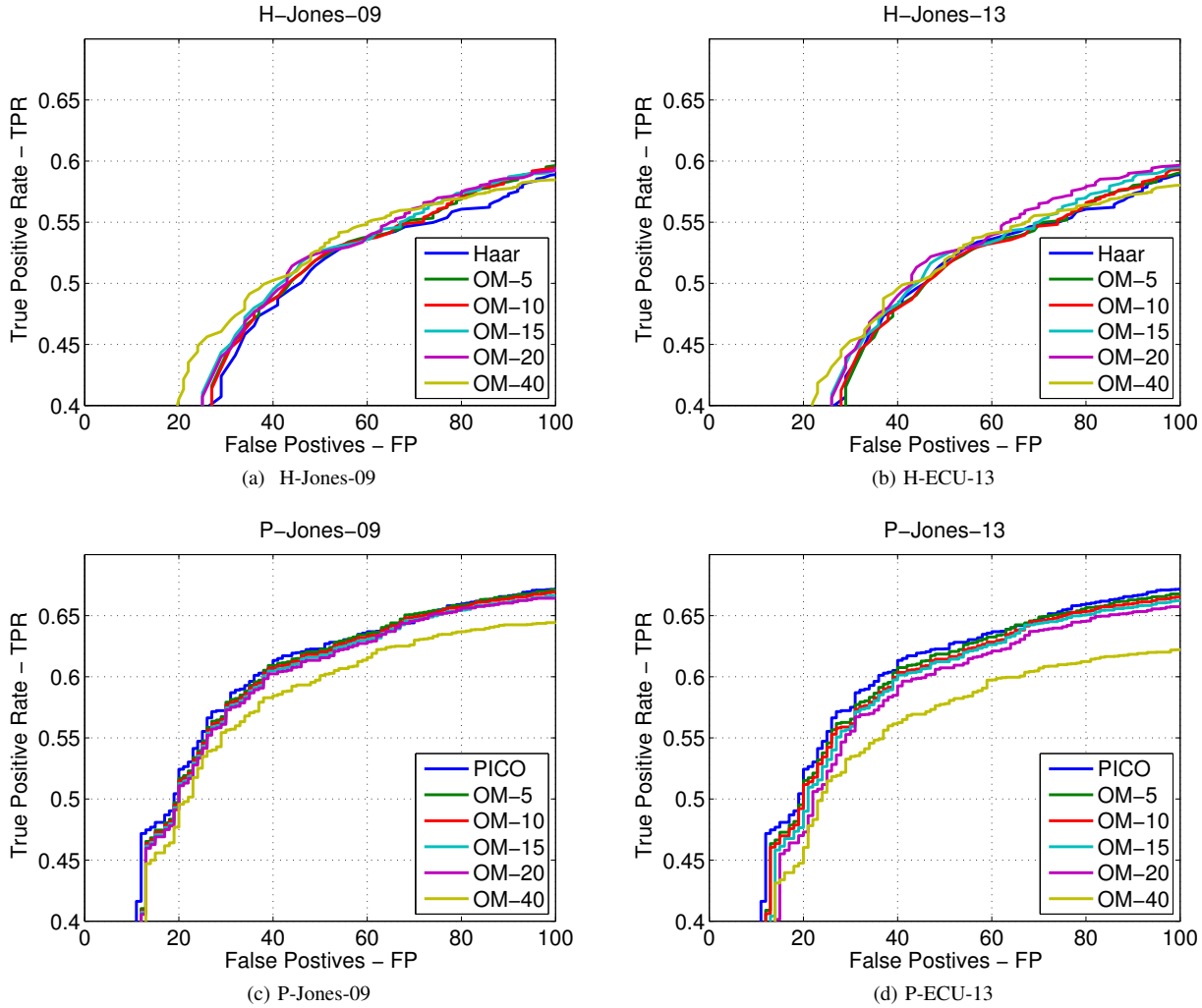

(a) H-Jones-09

(b) H-ECU-13

(c) P-Jones-09

(d) P-ECU-13

Fig. 4. ROC curves comparing our method with the references. As it is possible to see, our method for different values of Υ (SPT in the figure) shows similar performance to the reference, except for $\Upsilon = 40\%$

[4] K. Nallaperumal, S. Ravi, C. N. K. Babu, R. K. Selvakumar, A. L. Fred, S. Christopher, and S. S. Vinsley, "Skin detection using color pixel classification with application to face detection: A comparative study," in *Conference on Computational Intelligence and Multimedia Applications, 2007. International Conference on*, vol. 3, Dec 2007, pp. 436–441.

[5] L. Lang and W. Gu, "Study on face detection algorithm based on skin color segmentation and adaboost algorithm," in *Web Mining and Web-based Application, 2009. WMWA '09. Second Pacific-Asia Conference on*, June 2009, pp. 70–73.

[6] A. Kumar, "An empirical study of selection of the appropriate color space for skin detection: A case of face detection in color images," in *Issues and Challenges in Intelligent Computing Techniques (ICICT), 2014 International Conference on*, Feb 2014, pp. 725–730.

[7] W. Chen, K. Wang, H. Jiang, and M. Li, "Skin color modeling for face detection and segmentation: a review and a new approach," *Multimedia Tools and Applications*, vol. 75, no. 2, pp. 839–862, 2016.

[8] A. Koschan and M. A. Abidi, *Digital Color Image Processing*. New York, NY, USA: Wiley-Interscience, 2008.

[9] B. Muhammad and S. A. R. Abu-Bakar, "A hybrid skin color detection using hsv and ycgcr color space for face detection," in *2015 IEEE International Conference on Signal and Image Processing Applications (ICSIPA)*, Oct 2015, pp. 95–98.

[10] X. Wang, L. Wang, T. Lei, and C. Wang, "Face detection based on improved skin model and local iterated conditional modes," in *Natural Computation (ICNC), 2015 11th International Conference on*, Aug 2015, pp. 964–970.

[11] P. Viola and M. Jones, "Robust real-time face detection," *International Journal of Computer Vision*, vol. 57, pp. 137–154, May 2004.

[12] C. E. Erdem, S. Ulukaya, A. Karaali, and A. T. Erdem, "Combining haar feature and skin color based classifiers for face detection," in *2011 IEEE International Conference on Acoustics, Speech and Signal Processing (ICASSP)*, May 2011, pp. 1497–1500.

[13] J. Kovac, P. Peer, and F. Solina, "Human skin color clustering for face detection," in *The IEEE Region 8 EUROCON 2003. Computer as a Tool.*, vol. 2, Sept 2003, pp. 144–148 vol.2.

[14] S. L. Phung, A. Bouzerdoum, and D. Chai, "A novel skin color model in ycbcr color space and its application to human face detection," in *Proceedings. International Conference on Image Processing*, vol. 1, 2002, pp. I–289–I–292 vol.1.

[15] L. Zou and S. ichiro Kamata, "Face detection in color images based on skin color models," in *TENCON 2010 - 2010 IEEE Region 10 Conference*, 2010, pp. 681–686.

[16] S. Kherchaoui and A. Houacine, "Face detection based on a model of the skin color with constraints and template matching," in *Machine and Web Intelligence (ICMWI), 2010 International Conference on*, Oct 2010, pp. 469–472.

[17] G. C. Luh, "Face detection using combination of skin color pixel detection and viola-jones face detector," in *2014 International Conference on Machine Learning and Cybernetics*, vol. 1, July 2014, pp. 364–370.

[18] E. Mostafa, A. El-Barkouky, H. Rara, and A. Farag, "Rejecting pseudo-faces using the likelihood of facial features and skin," in *Biometrics:*

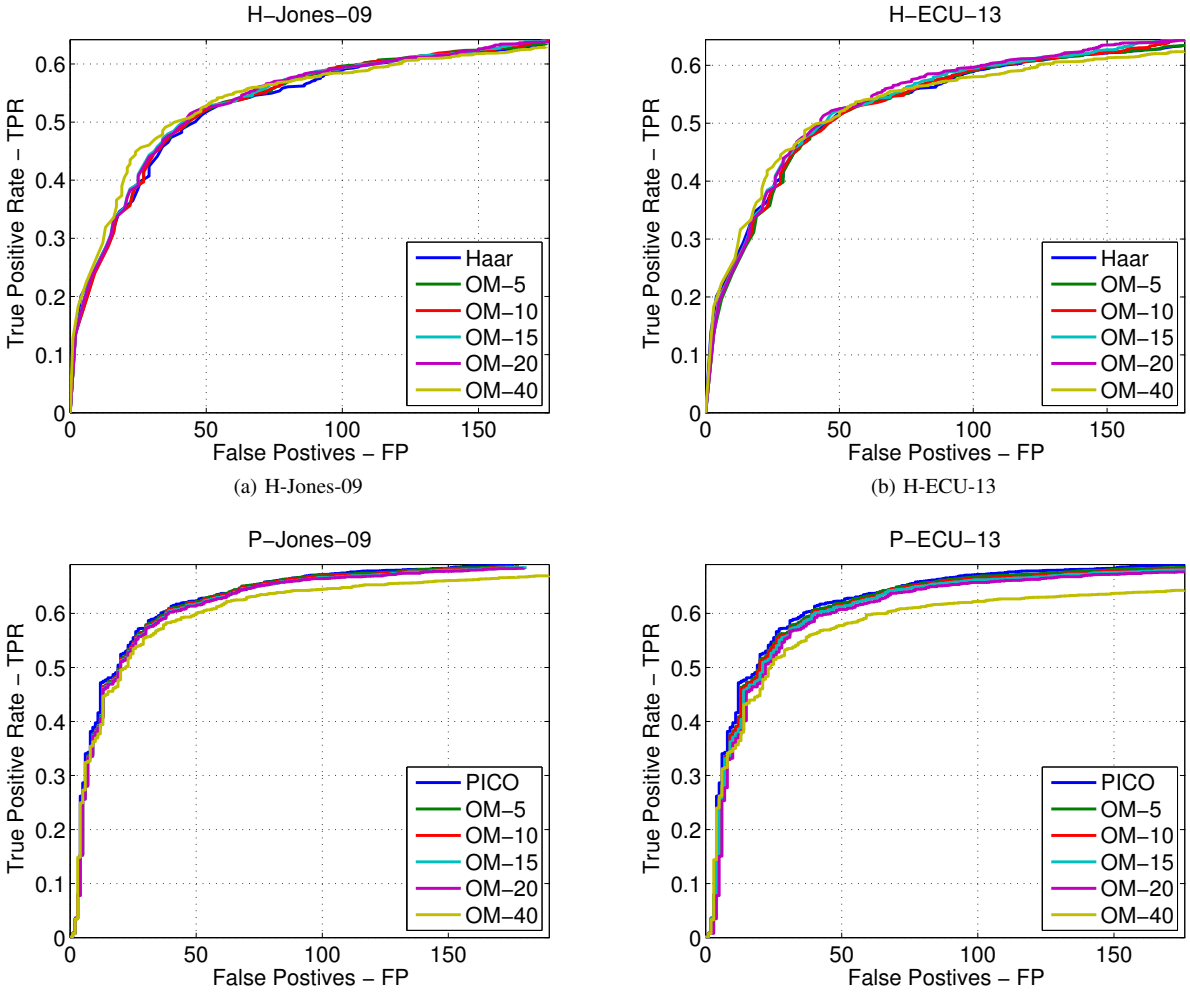

(a) H-Jones-09

(b) H-ECU-13

(c) P-Jones-09

(d) P-ECU-13

Fig. 5. Limited ROC curves used to calculate and compare the AUC of our method and the reference values. To limit the curves, in each plot, we chose the least number of False Positives when our method was applied.

Theory, Applications and Systems (BTAS), 2012 IEEE Fifth International Conference on, Sept 2012, pp. 365–370.

[19] Y. Ban, S.-K. Kim, S. Kim, K.-A. Toh, and S. Lee, "Face detection based on skin color likelihood," *Pattern Recognition*, vol. 47, no. 4, pp. 1573 – 1585, 2014.

[20] S. L. Phung, D. Chai, and A. Bouzerdoum, "Adaptive skin segmentation in color images," in *Multimedia and Expo, 2003. ICME '03. Proceedings. 2003 International Conference on*, vol. 3, July 2003, pp. III–173–6 vol.3.

[21] W. R. Tan, C. S. Chan, P. Yogarajah, and J. Condell, "A fusion approach for efficient human skin detection," *IEEE Transactions on Industrial Informatics*, vol. 8, no. 1, pp. 138–147, Feb 2012.

[22] X. Wang, H. Xu, H. Wang, and H. Li, "Robust real-time face detection with skin color detection and the modified census transform," in *Information and Automation, 2008. ICIA 2008. International Conference on*, June 2008, pp. 590–595.

[23] H. T. Ho and R. Chellappa, "Pose-invariant face recognition using markov random fields," *IEEE Transactions on Image Processing*, vol. 22, no. 4, pp. 1573–1584, April 2013.

[24] M. J. Jones and J. M. Rehg, "Statistical color models with application to skin detection," *International Journal of Computer Vision*, vol. 46, pp. 81–96, January 2002.

[25] V. Jain and E. Learned-Miller, "Fddb: A benchmark for face detection in unconstrained settings," University of Massachusetts, Amherst, Tech. Rep. UM-CS-2010-009, 2010.

[26] P. N. Belhumeur, D. W. Jacobs, D. J. Kriegman, and N. Kumar, "Localizing parts of faces using a consensus of exemplars," *IEEE Transactions on Pattern Analysis and Machine Intelligence*, vol. 35, no. 12, pp. 2930–2940, Dec 2013.

[27] N. Markus, M. Frljak, I. S. Pandzic, J. Ahlberg, and R. Forchheimer, "A method for object detection based on pixel intensity comparisons," *Computing Research Repository*, vol. abs/1305.4537, march 2013.

[28] S. Kang, B. Choi, and D. Jo, "Faces detection method based on skin color modeling," *Journal of Systems Architecture*, vol. 64, pp. 100 – 109, 2016, real-Time Signal Processing in Embedded Systems.

[29] M. H. Yang, D. J. Kriegman, and N. Ahuja, "Detecting faces in images: A survey," *IEEE Transactions on Pattern Analysis and Machine Intelligence*, vol. 24, pp. 34–58, January 2002.

[30] C. Papageorgiou, M. Oren, and T. Poggio, "A general framework for object detection," *International Conference on Computer Vision*, pp. 555–562, January 1998.

[31] M. Kawulok, J. Kawulok, and J. Nalepa, "Spatial-based skin detection using discriminative skin-presence features," *Pattern Recognition Letters*, vol. 41, pp. 3–13, May 2014.

[32] T. Fawcett, "An introduction to roc analysis," *In: Pattern Recognition Letters*, vol. 27, pp. 861–874, December 2005.

[33] T. Ojala, M. Pietikainen, and T. Maenpaa, "Multiresolution gray-scale and rotation invariant texture classification with local binary patterns," *IEEE Transactions on Pattern Analysis and Machine Intelligence*, vol. 24, no. 7, pp. 971–987, 2002.